Solid State Communications 269 (2018) 96–101

Contents lists available at ScienceDirect

Solid State Communications

journal homepage: www.elsevier.com/locate/ssc

Communication

High-pressure transformations of ortho-xylene probed by combined infrared and Raman spectroscopies

Yanzhi Bai [a], Nana Li [b], Cuiying Pei [b], Zhipeng Yan [b], Wentao Li [c], Dongqing Wei [a,*]

[a] *Department of Physics and Astronomy and College of Life Science and Biotechnology, Shanghai Jiaotong University, Shanghai 200240, China*
[b] *Center for High Pressure Science and Technology Advanced Research, Shanghai 201203, China*
[c] *Institute of Atomic and Molecular Physics, Sichuan University, Chengdu 610065, China*

ARTICLE INFO

Communicated by P. Sheng

Keywords:
A. Ortho-xylene
D. Phase transition and polymerization
E. Infrared and Raman spectroscopies
E. High pressure

ABSTRACT

Here, we report high-pressure investigations of ortho-xylene (o-xylene) using combined infrared (IR) and Raman spectral measurements at room temperature and pressures up to 32.1 GPa, respectively. Liquid o-xylene visually crystallized at around 0.4 GPa. Upon compression, the spectra changed; including splitting, disappearing, broadening of modes, and the appearance of new modes. We found four more phase transitions in o-xylene to phases III, IV, V, and VI at around 1.4, 3.9, 12.3, and 16.8 GPa, respectively. The final product recovered from over 20 GPa was preserved at ambient conditions and the mass spectrometry experiment indicated phase transition are polymerization.

1. Introduction

High-pressure techniques are an important tool in condensed matter chemistry, physics, and material science [1,2]. External pressure is able to tune the distance and the relative orientation among nearest neighbor molecules in materials. When suitable pressure conditions are achieved, a phase transition or chemical reaction can be induced in fluids or crystals of molecule-containing unsaturated bonds [3]. Many examples of such pressure-induced reactions or transformations have been reported in organic compounds. A phase change in solid benzene was observed around 11 GPa between phase III and III′, and a chemical reaction (V) at pressures above 23 GPa lead to the formation of saturated carbon atoms [4]. Mario Santoro et al. [3] observed that acetylene polymerized at 4 GPa after a 42 h reaction through an infrared absorption experiment in the region 600-1800 cm^{-1}. Formic Acid (HCOOH) was also found to transform into a polymeric amorphous phase at 40 GPa using Raman, IR, and X-ray diffraction (XRD) measurements [5]. Phase transformations of thiophene (C4H4S) [6] and benzene [7] were studied visually and with IR up to 30 GPa, and transformed to polymer conditions around 20 GPa.

Raman spectroscopy is one of the most promising spectroscopic methods due to its fast response and ability to monitor the progress of reactions with continuously timed observations of the chemical engineering-induced variation of peaks [8–10]. Infrared (IR) spectra also provide a powerful method for probing certain aspects of molecular structures and intramolecular forces [11,12]. O-xylene, as a typical organic compound, has been widely used as a chemical raw material and solvent to produce phthalic anhydride and synthesize other raw organic materials for example, manufacturing paints, synthetic rubbers, adhesives, degreasing agents, and agricultural chemicals, etc.

To date, investigations of liquid o-xylene using infrared [13], Raman [14], and neutron scattering [15] techniques under ambient conditions have been reported. However, the properties of o-xylene under high pressure have not been studied. Where pressure is concerned, liquid-solid and solid-solid phase transitions generally precede dramatic electronic changes such as molecular-non-molecular transformations or irreversible chemical reactions. This could improve the synthesis of new materials using high-pressure technology. Therefore, it is instructive to study o-xylene extensively for potential industrial applications and scientific research. Here, we investigated the high-pressure vibrational spectroscopic behaviors of o-xylene with IR and Raman spectroscopy.

In this work, we conducted high-pressure IR and Raman measurements of o-xylene at room temperature with a diamond anvil cell (DAC) up to ≈32 GPa. We discuss our preliminary results on the pressure effect on the transformation and properties of o-xylene, revealing its phase transition using its vibrational spectrum. The decompressed samples were also investigated by mass spectrometry (MS) experiment.

---

[*] Corresponding author.
E-mail address: dqwei@sjtu.edu.cn (D. Wei).

https://doi.org/10.1016/j.ssc.2017.09.022
Received 29 August 2017; Accepted 27 September 2017

2. Experimental

In situ high-pressure investigations were performed with a DAC in all experiments. The cell was loaded by filling the gasket hole with a drop of liquid o-xylene from Alfa Aesar Puratonic (purity ≥ 99.9%). Gaskets with a diameter of 120 μm and thickness of 40–50 μm served as the initial sample chambers. Ruby balls were inserted in the sample to measure the local sample pressure by the R1 ruby fluorescence band shift [16]. A Fourier transform IR spectrometer (Bruker Vertex80 V FTIR) was used to measure the IR absorption spectra. The instrument was equipped with different beam splitters and detectors to cover the frequencies from 400 to 4000 cm^{-1}. Raman spectra were measured using the 532 nm line of a He/Ne laser excitation source at frequencies of 80–3500 cm^{-1}, with an instrumental resolution better than 1 cm^{-1}. All experiments were conducted at room temperature from 24 °C to 28 °C. The MS experiment was performed by matrix-assisted laser desorption/ionization time-of-flight mass spectrometry (MALDI-TOF-MS) with DCTB 2-[(2E)-3-(4-tert-butylphenyl)-2-methylprop-2-enylidene] malononitrile and dithranol as matrix, respectively.

3. Results and discussion

3.1. Visual observation

High-pressure crystallization of liquids has been known as an alternative to crystallization at low-temperature since the 1950s [17–19]. Here, visual observations of o-xylene were performed at room temperature with a microscope in a DAC. After inserting ruby balls for pressure calibration and filling the chamber with liquid o-xylene, the pressure was gradually increased. The liquid completely solidified into a crystalline state when the pressure exceeded the freezing pressure of liquid o-xylene. With careful manipulation of the DAC by repeated compression and decompression, the o-xylene formed the single crystal shown in Fig. 1. The crystallization pressure was determined at 0.4 GPa and room temperature, where the solid and liquid phase coexisted; crystal phase II.

3.2. IR spectra upon compression

First, we collected the IR spectra when the sample was loaded into the DAC. Our experimental IR spectra excellently agree with the Sadtler standard IR spectroscopy and calculation result. In order to facilitate the assignment and description of the experimental vibration modes, we list the corresponding positions and assignments of the bands under ambient conditions in Table 1. The bond assignments were based on our calculations with the DFT method and literature on the IR characteristic group frequencies [20–23]. In this table, we did not include any of the new modes that appeared in the new phase. However, the nature of the new modes can be assigned by correlating their origin to the corresponding mode in the ambient phase.

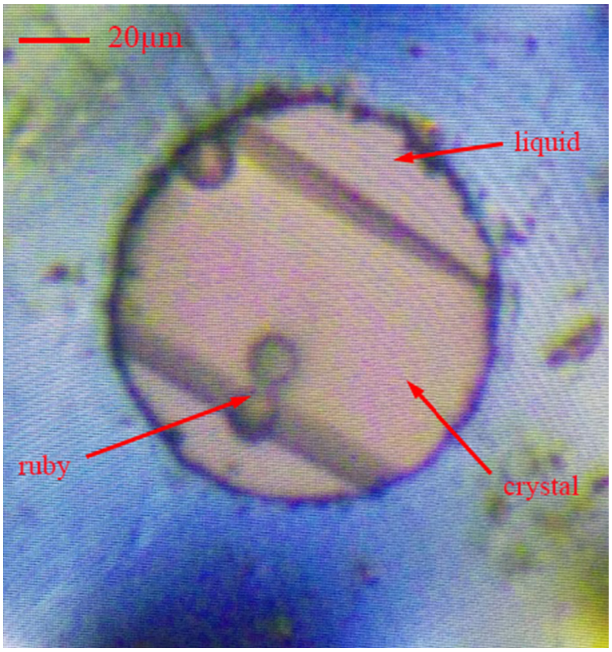

Fig. 1. A view of the DAC high-pressure chamber with the pressure-induced single crystal of o-xylene. Three ruby balls for pressure calibration are located in the chamber.

We collected IR spectra from 600 to 3400 cm^{-1} and up to 32.1 GPa. In the spectra, the strongest absorptions for aromatic compounds occur between 650 and 900 cm^{-1} and the bands in this region are assigned to the C=C and C—H vibrations with out-of-plane bending of the benzene ring [24]. A number of higher frequency bands appeared between 900 and 1290 cm^{-1}, or the fingerprint area. For o-xylene, the fingerprint area mainly involved CH_3 stretching and C—H angular vibration modes. The intensity bonds in the region 1430-1625 cm^{-1} mainly originated from ring carbon-carbon (C=C) stretching and C—H angular vibration. The bands in the region 2850-3106 cm^{-1} are associated with the C—H vibrational of the methyl and benzene ring.

The selected IR spectra as a function of pressure are presented in Fig. 2, which shows that, at 1.4 GPa, two small splits (marked by •) occurred at the lower-frequency side and higher-frequency side of the bands 757 and 3082 cm^{-1}, respectively. Also, the band at 1470 cm^{-1} disappeared when o-xylene was compressed from 0.3 GPa to 1.4 GPa. The spectra changes mainly involved the stretching vibrational modes of C=C, CH_3 and C—H, corresponding to the phase transition from phase II → III. To better interpret the spectral changes and understand the transition boundaries during pressure increase, the pressure dependence of all the IR frequency are also plotted and shown in Fig. 3. The effects of pressure on the vibrational modes in this region can be seen around 1.4 GPa.

Upon further compression to 3.9 GPa, we observed considerable changes in the spectrum, such as the splitting and disappearance of the existing modes together with appearance of new modes. During compression from 1.4 to 3.9 GPa, the broad band centered at 935 cm^{-1} started to separate into two modes at 937 and 946 cm^{-1} (see the enlarged spectra at 3.9 GPa in Fig. 2a). Furthermore, a new, clear peak occurred at 1052 cm^{-1} (see Fig. 2a, marked by *) and the peak at 3114 cm^{-1} disappeared (see Fig. 3c). In Fig. 2b, changes mainly involved band appearance and disappearance or intensity variation of the bands assigned to CH_3 and C—H stretching.

The electrical forces associated with intermolecular interaction are usually much weaker than the intramolecular forces [25–27]. We might expect the molecular modes and their frequencies to be altered relatively when the molecules in the liquid phase are compressed to a crystalline state or as a function of the crystallinity. Therefore, the observed intensity increase of the new bands could be related to a transition by further crystallization of o-xylene [28] as the sample changed to another phase. These prominent changes of band splitting, appearance, disappearance and intensity changes indicate that o-xylene underwent a new crystal phase transformation from III → IV during compression to 3.9 GPa.

As the pressure increased in phase IV (3.9 GPa), we observed significant changes in C—H and C=C vibrational modes in the IR spectra. The peaks broadened and merged between 1420 and 1580 cm^{-1} at 8.3 GPa, indicating that the pressure-induced changes first involved C=C ring stretching (see Fig. 2 at 8.3 GPa). As shown in Fig. 3a, a bond at 967 cm^{-1} assigned to the C—H ring mode disappeared and the mode at 987 cm^{-1} increased at a rate of 1.0 cm^{-1}/GPa until 12.3 GPa. From 2800 to 3250 cm^{-1}, the vibrations mainly involved the C—H modes and at around 12.3 GPa, band splitting and a clear new peak emerged at 2978 and 3240 cm^{-1}, respectively. The splitting of the peak suggests that o-xylene changed to another different crystalline component. The new peak that appeared around 2979 and 3238 cm^{-1} suggests new C—H band

Table 1
Vibrational Frequencies (cm^{-1}) of o-xylene and Normal mode Description.

Sadtler Standard IR Spectroscopy[a]	calculated[b]	experimental[c]	normal mode description
742 (s)	721.1(0.0), 722.9(64.7)	750.5(s)	υ(C⎓C + CH_3)
	805.1(0.8), 841.3(0.0)	825(w)	ω(C—H) of ring
	894.9(0.9)	859(w)	ω(C—H) of ring
932(w)	933.1(0.0)	933.4(w)	ω(C—H) of ring
985(m)	977.4(2.7), 981.4(2.7)	989(m)	ω(CH_3)
1022(m)	1017.6(10.6)	1023.5(s)	
1053(s)	1039.8(42.8), 1043(0.0)	1055(s)	ω(C—H)
1120(m)	1105.6(10.0)	1121(w)	ω(C—H)of (ring + CH_3)
1146(w)	1145.9(0.4)		ω(C—H)
1157(w)	1164.3(0.1)	1156(w)	ω(C—H)of ring+υ(CH_3)
1186(w)		1187(w)	
1223(m)	1205.9(15.1)	1224(w)	ω(C—H)of ring+υ(CH_3)
1291(w)	1275.1(1.1), 1296.6(0.4)	1291.6(w)	υ(C⎓C)
1384(m)	1387.8(2.4), 1398.8(7.5)	1381(w)	ω(C—H) of CH_3
	1428.8(0.0)		υ(C—H) of ring
	1449.0(0.0)	1446(s)	ω(C—H) of CH_3
1456(s)	1463.1(27.2)	1459(s)	ω(C—H) of CH_3
1467(s)	1464.0(4.4),1465.8(98.1)	1470(s)	ω(C—H) of CH_3
	1480.6(94.0)	1483(s)	υ(C⎓C)
1495(s)		1496(s)	
1583(m)	1573.4(2.0)	1583(w)	ω(C—H)+υ(C⎓C) of ring
1606(m)	1601.7(16.5)	1606(w)	ω(C—H)+υ(C⎓C) of ring
1787(w)		1797.2(w)	
1901(m)		1906.8(w)	
1942(w)		1949.6(w)	
2732(m)			
2860(m)		2859(m)	
2878(m)		2881.5(m)	
2921(s)	2922.4(262.1),2924.0(37.9)	2922.4(s)	υ(C—H) of CH_3
2940(s)		2943(s)	υ(C—H) of CH_3
2971(s)	2969.3(55.2),2972.1(0.0)	2972.5(s)	υ(C—H) of CH_3
3018(s)	3003.1(195.9),3006.8(15.4)	3016(s)	υ(C—H) of CH_3
3050(m)	3042.2(12.6),3049.7(81.9)	3049(m)	υ(C—H) of ring
3066(m)	3057.3(257.3),3057.4(233.3)	3068.1(s)	υ(C—H) of ring
3108(m)		3106(m)	υ(C—H) of ring

υ: stretching; γ: in-plane-bend; ρ: in-plane-bend; ω: variable angular vibration.

[a] Calculated from the o-xylene liquid phase with the Onsager method (B3LYP/6-31G).

[b] Infrared spectra from the Sadtler spectroscopy database.

[c] This work (ambient temperature and ≈0.3 GPa).

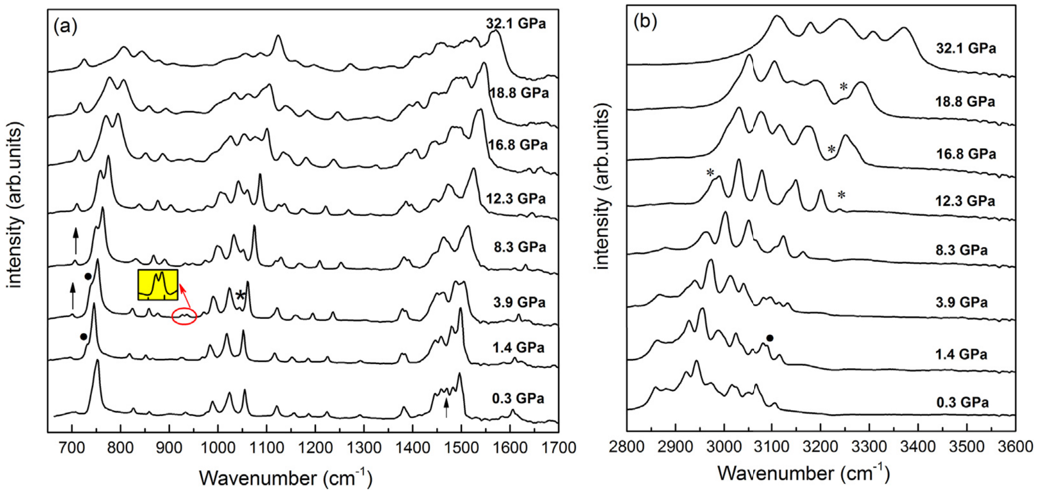

Fig. 2. IR spectrum of o-xylene over 600-3400 cm^{-1} with increasing pressure. Arrows (↑) around 700 cm^{-1} indicate the peaks that increased in intensity. Arrows (↓) indicate the peak that disappeared under compression to 1.4 GPa. The * signed new peaks appeared and the full dots • symbol shows the band splitting. The yellow area is the enlargement of the spectrum at 937 and 946 cm^{-1} at 3.9 GPa. (For interpretation of the references to colour in this figure legend, the reader is referred to the web version of this article.)

formation and that a high-pressure reaction lead to the formation of new phase products. These could, in turn, be related to the new crystalline phase IV→V, which appeared above 12.3 GPa.

Upon further compression to 16.8 GPa, the IR spectra was characterized by extreme band broadening and merging, as well as the disappearing of weak bands (e.g. 943, 957, 1060 cm^{-1}) belonging to the intermolecular interaction. As shown in Fig. 2b, three new peaks appeared around 1500 cm^{-1}, which related to the C—H and C═C vibration (See Fig. 3b). A new weak peak was also observed at 3224 cm^{-1} (See Fig. 2b at 16.8 GPa and Fig. 3c), which was assigned to the C—H ring vibrational modes and their intensity increased as pressure increased. These phenomena all indicate a phase transition from V→VI at 16.8 GPa.

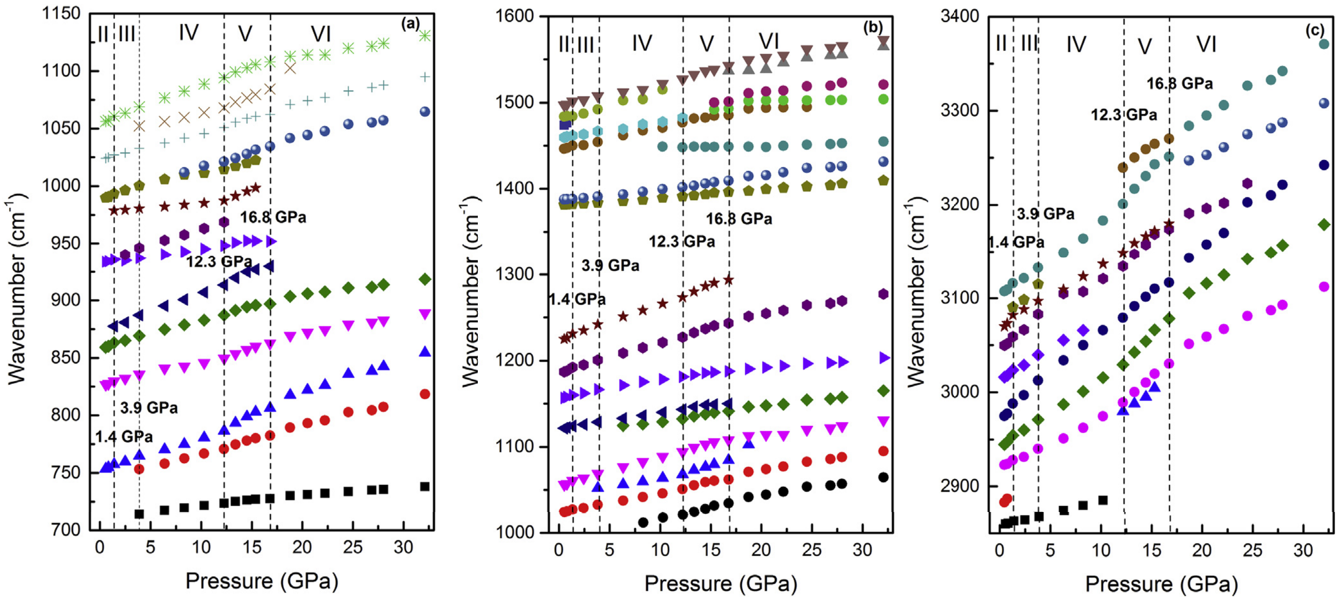

Fig. 3. Change in frequency of the vibrational of o-xylene over 700-1150 cm^{-1}, 1000-1600 cm^{-1}, and 2850-3400 cm^{-1}, as a function of pressure.

These changes mainly involved new C—H bonds formation and band broadening, suggesting the new phase could be more strained and amorphous. The IR spectrum patterns at 18.8 GPa was preserved up to 32.1 GPa, the highest pressure applied in our experiment, as shown in Fig. 2.

In the IR spectrum, o-xylene underwent a series of transitions as the pressure increased up to ≈32 GPa. We performed a single-crystal X-ray diffraction experiment in a DAC and also tried to determine the high-pressure structure (atomic positions) by using the GSE_ADA program (Dera et al., 2009). Unfortunately, due to the limitation of the DAC opening angle, we could not obtain the detailed structure of o-xylene. In order to confirm the conclusion of our IR spectra, we also collected Raman spectra upon compression to 30.8 GPa. In the spectrum, we observed the corresponding Raman changes at these pressures, confirming the IR results.

3.3. Raman spectra upon compression

Selected Raman spectra of o-xylene under compression to 30.8 GPa are depicted in Fig. 4. The first-order diamond Raman band is omitted for clarity. Upon compression, all the vibrational modes shifted monotonically to higher frequencies. Fig. 4 shows that there was no considerable change at 0.4 GPa, possibly because the laser hit the liquid region, where the liquid and crystal coexist at around 0.4 GPa. As the pressure increased up to 1.3 GPa, two new Raman modes in the lattice region were observed at 122 and 132 cm^{-1} (see Fig. 4a). In Fig. 4b, another new peak was observed at 749 cm^{-1}. Furthermore, a few weak peaks appeared around 1165 and 3000 cm^{-1} (See Fig. 5a and b), which could be attributed to the intermolecular interaction changes in the crystallized phase III. This is consistent with the IR observation that o-xylene underwent a new crystallized phase transformation (phase III) under compression to 1.4 GPa.

Upon further compression, most of the characteristic crystalline o-xylene lattice modes gradually lost intensity and broadened. However, a new mode appeared at 91 cm^{-1} in the lattice region and the sharp peak at 583 cm^{-1} changed to a weak, broad band when o-xylene was compressed from 1.3 to 3.5 GPa. At the low-frequency side of the mode 1065 cm^{-1}(See Fig. 5a), a very weak peak was observed and increased in intensity when compressed towards higher pressure. In Fig. 5b, a clear splitting occurred at 2943 cm^{-1} and the intensity reversed during compression. Therefore, it is likely that a phase IV transition occurred around 3.5 GPa, which is consistent with our IR observation. As the pressure increased in phase IV, we observed a clear new mode at 91 cm^{-1} in the lattice mode region (See Fig. 4a) and the broad band split into a double band (centered at 585 and 591 cm^{-1}) at 5.5 GPa (See Fig. 4b). All lattice modes broadened and decreased during further compression up to 12.3 GPa. There was a shoulder splitting at the low-frequency side of mode at 1281 cm^{-1} and the peak at 3068 cm^{-1} disappeared, as shown in Fig. 5a and b, respectively. The splitting of the peaks already there should suggested different crystalline (Davydov) components (phase V) of o-xylene.

Above 16.8 GPa, the lattice modes disappeared (See Fig. 4a) and only a few vibration modes preserved. The frequencies in the region of 2800–3400 cm^{-1} are usually assigned to C—H and CH_3 stretching modes. The bands broadened and weakened in intensity. In our experiments no

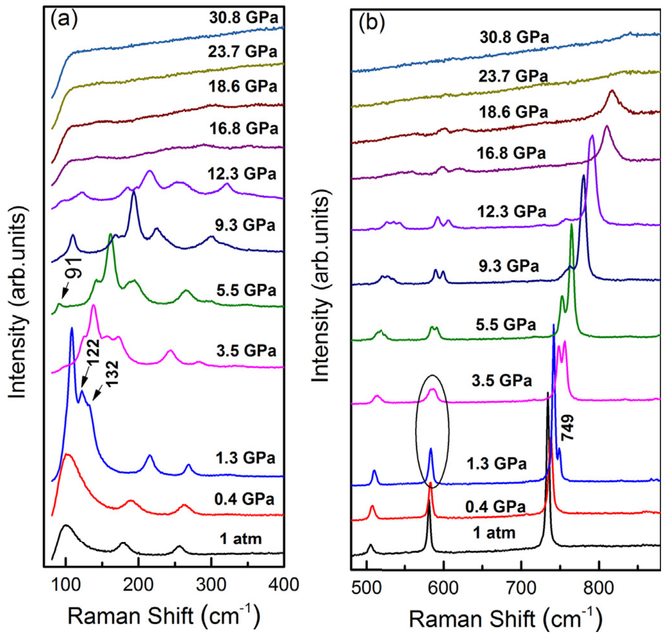

Fig. 4. Selected high-pressure Raman spectra of o-xylene in the region of (a) 80–400 cm^{-1} and (b) 480-880 cm^{-1}. The numbers are the peak position and the unit is cm^{-1}. The comparison of the peak 580 cm^{-1} between 1.3 and 3.5 GPa is shown in the rectangle.

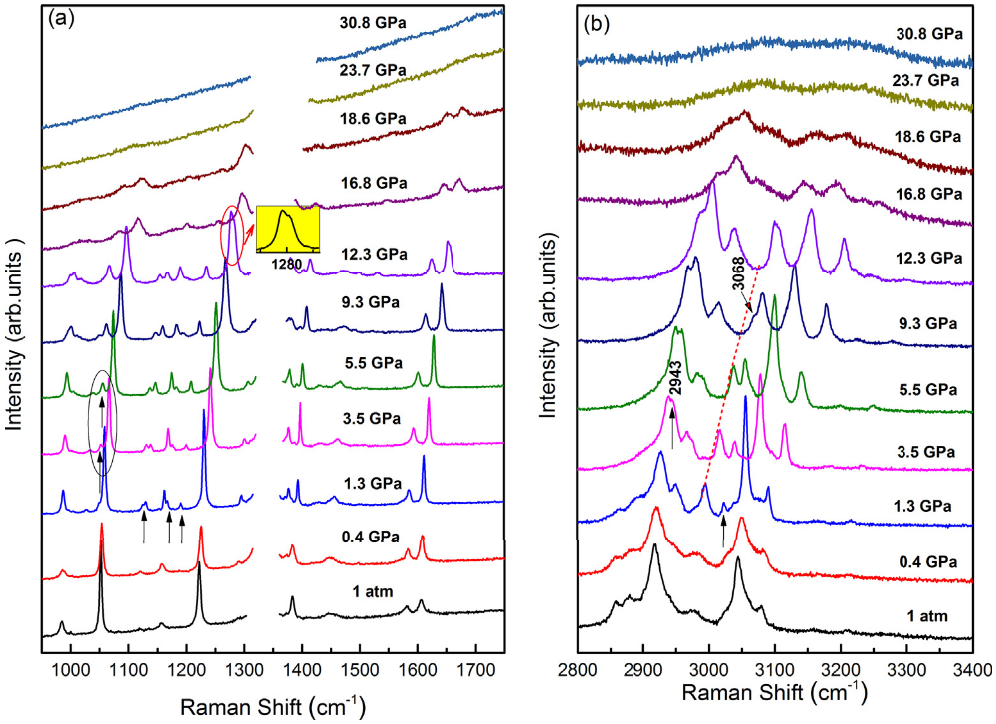

Fig. 5. Selected high-pressure Raman spectra of o-xylene in the region of (a) 950–1750 cm^{-1} and (b) 2800-3400 cm^{-1}. The omitted spectral regions (around 1350 cm^{-1}) are due to the diamond. The numbers are the peak position and the unit is cm^{-1}. The comparison of the peak around 1052 cm^{-1} between 3.5 and 5.5 GPa is shown in the oval. All the symbols ↑ show new peaks or peak splitting. The enlargement of the splitting at 1280 cm^{-1} is shown in a yellow rectangle. The dashed line indicates the evolution of the band at 3068 cm^{-1}. (For interpretation of the references to colour in this figure legend, the reader is referred to the web version of this article.)

pressure-transmitting medium was used, suggesting that the broad Raman bands in Fig. 5b were primarily due to a new phase with a more disordered lattice. This result is consistent with the IR observation that a new phase change (VI) occurred at 16.8 GPa.

Thus, we observed a series of transitions during the compression of o-xylene up to around 32 GPa. Our IR and Raman scattering results can be summarized as follows:

$$\text{Phase I}\xrightarrow{\approx 0.4\text{GPa}}\text{Phase II}\xrightarrow{1.3\text{GPa}}\text{Phase III}\xrightarrow{3.9\text{GPa}}\text{Phase IV}\xrightarrow{12.3\text{GPa}}\text{Phase V}\xrightarrow{16.8\text{GPa}}\text{Phase VI}$$

3.4. *Physicochemical properties of the recovered products*

In order to obtain an intuitive observation of the products around 20 GPa, we performed more independent experiments and compressed o-xylene at different pressures. We found that under 20 GPa, a monomer still presented in the cell, a sheet of liquid appeared between the diamond culet, and the sample rapidly evaporated (See Fig. 6a), which indicates an incomplete reaction. However, for the sample compressed above 20 GPa, a considerable amount of white/transparent plastic solid was recovered at ambient conditions (See Fig. 6b), which suggests the final transition can be preserved under ambient conditions.

We also performed MALDI-TOF/MS to investigate the recovered products. The experiments were performed with DCTB and dithranol matrixes and the samples were recovered from ~25.6 GPa to ambient conditions. From the mass spectrum, a number of mass-to-charge (m/z, m is the mass and z is charge) occurred at m/z 437, 481(473), 628(619), and 650(647) as shown in Fig. 7. Through analysis, we found that the m/z value of an oligomer is not exactly the integral multiple of the mass number of the C_8H_{10} monomer. The isomeric adjustment and random copolymerization make the m/z of the polymer different. However, the

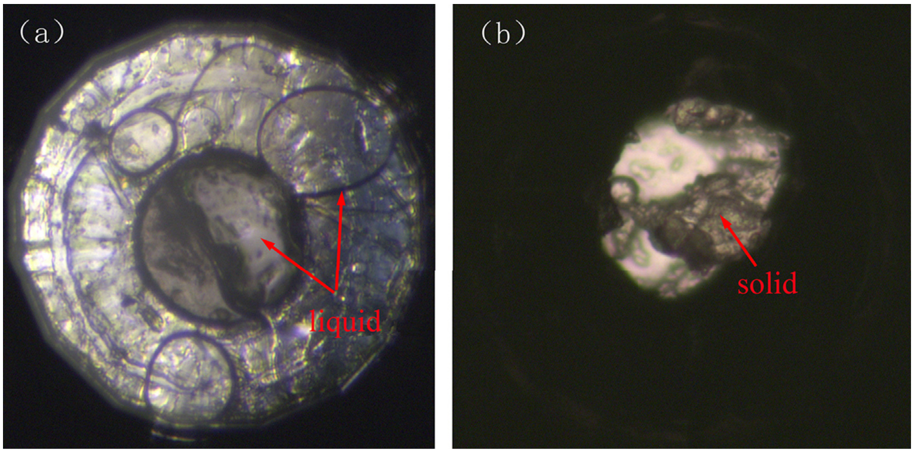

Fig. 6. The final products of o-xylene that recovered from around (a) 15 GPa and (b) 21 GPa, respectively.

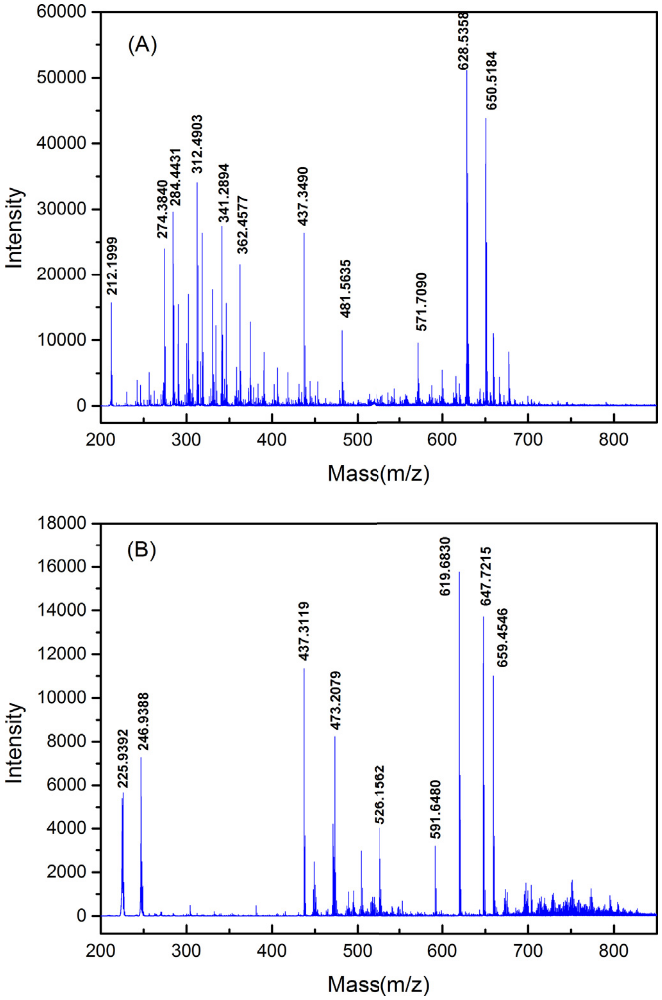

Fig. 7. MAlDI-TOF/MS spectrum of o-xylene that decompressed from ~25.6 GPa. (A) Spectrum acquired using DCTB as the matrix; and (B) Spectrum acquired using dithranol as matrix.

oligomers mainly involved tetramer and hexamer polymers. Therefore, we conclude that the application of pressure up to 16.8 GPa does lead to a new crystalline polymerized phase transformation of o-xylene.

4. Conclusions

Our high-pressure IR and Raman investigations of o-xylene from 32 and 31.8 GPa suggest the existence of five pressure-induced phase transitions at around 0.4, 1.4, 3.9, 12.3, and 16.8 GPa. O-xylene crystallized at around 0.4 GPa. The emergence of several new modes, splitting of existing modes, disappearance, and also intensity changes for serval modes indicated the phase III and IV transition at 1.4 and 3.9 GPa, respectively. At 12.3 GPa, both IR and Raman characterized the spectrum by broadening and splitting, indicating another crystalline transition from phase IV to V at 12.3 GPa. The band broadening and merging, as well as the appearance of weak bands at around 16.8 GPa, suggested polymerized phase VI formation and verified by the mass spectrometry investigation on the decompressed samples.

Acknowledgments

We would like to thank Center for High Pressure Science and Technology Advanced Research for high pressure experiments support and the professor of Lin Wang. The IR experiments were performed at State Key Laboratory of Superhard Materials of Jilin University. This work was partially supported by Natural Science Foundation of China (Grant No. 11004072 and 11174201). This work is also partially supported by the Science Challenge Program, No. TZ2016001 and the State Key Laboratory of Explosion Science and Technology, Beijing Institute of Technology (KFJJ15).

References

[1] D. Chelazzi, M. Ceppatelli, M. Santoro, R. Bini, V. Schettino, Nat. Mater. 3 (2004) 470–475.
[2] M. Citroni, M. Ceppatelli, R. Bini, V. Schettino, Science 295 (2002) 2058–2060.
[3] M. Santoro, L. Ciabini, R. Bini, V. Schettino, J. Raman Spectrosc. 34 (2003) 557–566.
[4] L. Ciabini, M. Santoro, R. Bini, V. Schettino, J. Chem. Phys. 115 (2001) 3742–3749.
[5] A.F. Goncharov, M.R. Manaa, J.M. Zaug, R.H. Gee, L.E. Fried, W.B. Montgomery, Phys. Rev. Lett. 94 (2005) 065505–065508.
[6] Ph. Pruzan, J.C. Chervin, J.P. Forgerit, J. Chem. Phys. 96 (1992) 761–767.
[7] Ph. Pruzan, J.C. Chervin, M.M. Thiery, J.P. Itie, J.M. Besson, J.P. Forgerit, M. Revault, J. Chem. Phys. 92 (1990) 6910–6915.
[8] U.D. Venkateswaran, E.A. Brandsen, M.E. Katakowski, Phys. Rev. B 65 (2002) 054102–054107.
[9] M.J. Peters, Phys. Rev. B 61 (2000) 5939–5944.
[10] V. Iota, C.S. Yoo, J.H. Klepeis, Z. Jenei, W. Evans, H. Cynn, Nat. Mater. 6 (2007) 34–38.
[11] A.M. Rao, P.C. Eklund, J.L. Hodeau, L. Marques, M. Nunez-Regueiro, Phys. Rev. B 55 (1997) 4766–4773.
[12] J.R. Durig, W.H. Green, W.H. Hammond, J. Phys. Chem. 70 (1966) 1989–1997.
[13] C.J.M. Chin, L.C. Shih, H.J. Tsai, T.K. Liu, Carbon 45 (2007) 1254–1260.
[14] N. Wright, P. Stout, K. Krishnan, Fresenius J. Anal. Chem. 339 (1991) 271–275.
[15] K.C. Ingham, S.J. Strickler, J. Chem. Phys. 53 (1970) 4313–4318.
[16] H.K. Mao, J. Xu, P.M. Bell, J. Geophys. Res. 91 (1986) 4673–4676.
[17] P.W. Bridgman, Rev. Mod. Phys. 18 (1946) 1–93.
[18] P.W. Bridgman, The Physics of High Pressure, vol. 56, Bell and Sons, London, or Macmillan, New York, 1931.
[19] E.V. Boldyreva, Acta Cryst. A 64 (2008) 218–231.
[20] J. Coates, Interpretation of Infrared Spectra, a Practical Approach. Encyclopedia of Analytical Chemistry, 2000.
[21] G. Varsanyi, Vibrational Spectra of Benzene Derivatives, New York, 1969.
[22] L. Ciabini, M. Santoro, R. Bini, V. Schettino, J. Phys. Chem. 116 (2002) 2928–2935.
[23] A. Banerji, S.K. Deb, J. Phys. Chem. B 111 (2007) 10915–10919.
[24] T.F. Ardyukova, Atlas of Spectra of Aromatic and Hererocyclic Compounds, Nauka Sib. Otd., Novosibirsk, 1973.
[25] J.D. Dunitz, G. Angelo, Chem. Soc. Rev. 38 (2009) 2622–2633.
[26] L. Colombo, P. Bleckmann, B. Schrader, R. Schneider, T. Plesser, J. Chem. Phys. 61 (1974) 3270–3278.
[27] K.N. Baker, A.V. Fratini, R. Timothy, H.C. Knachel, W.W. Adams, E.P. Socci, B.L. Farmer, Polymer 34 (1993) 1571–1587.
[28] Z. Jianming, T. Hideto, N. Isao, O. Yukihiro, Macromol 37 (2004) 6433–6439.